Research Article

Tectonics and sedimentation around Kashinosaki Knoll: A subducting basement high in the eastern Nankai Trough

Toshihiro Ike,[1] Gregory F. Moore,[1,2,*] Shin'ichi Kuramoto,[2] Jin-Oh Park,[3,†] Yoshiyuki Kaneda[3] and Asahiko Taira[2]

[1]*Department of Geology and Geophysics, University of Hawai'i, Honolulu, HI 96822, USA,* [2]*Center for Deep Earth Exploration, JAMSTEC, Yokohama, Kanagawa 236-0001, Japan, and* [3]*Institute For Research on Earth Evolution, JAMSTEC, Yokohama, Kanagawa 237-0001, Japan*

Abstract   When seamounts and other topographic highs on an oceanic plate are subducted, they cause significant deformation of the overriding plate and may act as asperities deeper in the seismogenic zone. Kashinosaki Knoll (KK) is an isolated basement high of volcanic origin on the subducting Philippine Sea Plate that will soon be subducted at the eastern Nankai Trough. Seismic reflection imaging reveals a thick accumulation of sediments (~1200 m) over and around the knoll. The lower portion of the sedimentary section has a package of high-amplitude, continuous reflections, interpreted as turbidites, that lap onto steep basement slopes but are parallel to the gentler basement slopes. Total sediment thickness on the western and northern slopes is approximately 40–50% more than on the summit and southeastern slopes of KK. These characteristics imply that the basal sedimentary section northwest of KK was deposited by infrequent high-energy turbidity currents, whereas the area southeast of KK was dominated by hemipelagic sedimentation over asymmetric basement relief. From the sediment structure and magnetic anomalies, we estimate that the knoll likely formed near the spreading center of the Shikoku Basin in the early Miocene. Its origin differs from that of nearby Zenisu Ridge, which is a piece of the Shikoku Basin crust uplifted along a thrust fault related to the collision of the Izu–Bonin arc and Honshu. KK has been carried into the margin of the Nankai Trough, and its high topography is deflecting Quaternary trench turbidites to the south. When KK collides with the accretionary prism in about 1 My, the associated variations in sediment type and thickness around the knoll will likely result in complex local variations in prism deformation.

Key words: Nankai Trough, ridge subduction, turbidite sedimentation.

INTRODUCTION

The subduction of seamounts, fracture zones, and aseismic ridges at convergent margins causes significant deformation of the overriding plate

*Correspondence: Department of Geology and Geophysics, 1680 East-West Road, University of Hawaii, Honolulu, HI 96822, USA (email: gmoore@hawaii.edu).

†Present address: Ocean Research Institute, University of Tokyo, Nakano, Tokyo, 164-8639, Japan.

(Cadet *et al.* 1987; Kobayashi *et al.* 1987; McCann & Habermann 1989; Dominguez *et al.* 1998, 2000; Kodaira *et al.* 2000; von Huene *et al.* 2000; Taylor *et al.* 2005). At margins with voluminous trench sediment supply, the introduction of these topographic highs into the trench disrupts the normal flow of trench turbidites, causing significant along-strike variations in sediment thickness and type entering the subduction zone (Underwood *et al.* 1993; Alexander & Morris 1994). This in turn leads to potential lateral variations in pore fluid pressure that can further affect accretionary processes

(e.g. Saffer & Bekins 2002; Spinelli & Underwood 2004). Moreover, these bathymetric features are likely to act as asperities when they are carried to deeper levels of the subduction zone (Cloos & Shreve 1996; Scholz & Small 1997).

The Nankai Trough, south of Japan, is the site of on-going seamount subduction, as evidenced by several large and small embayments in the forearc (Okino & Kato 1995). The largest of these is directly in line with the Kinan Seamount Chain (KSC; Fig. 1a insert) on the subducting Philippine Sea Plate (PSP; Yamazaki & Okamura 1989), and a subducted seamount in this region has been identified (Kodaira *et al.* 2000). Collision of the Zenisu Ridge (ZR) and paleo-Zenisu Ridge has caused massive modification to the Nankai accretionary prism farther to the NE (Le Pichon *et al.* 1987). On the PSP, south of the Kumano Basin, there is a large topographic high, Kashinosaki Knoll (KK) that is currently just outboard of the Nankai Trough axis (Fig. 1a). This knoll has been interpreted to be part of the ZR complex farther to the northeast (Aoki *et al.* 1982; Lallemant *et al.* 1989), but it may be an isolated seamount not connected to any other ridges.

As part of the Nankai Trough Seismogenic Zone Experiment (NanTroSEIZE), we recently collected many new seismic reflection lines and swath bathymetric data to formulate a better understanding of the structure and stratigraphy of the Kumano Basin section of the Nankai Trough. Here we present an analysis of those data sets aimed at defining the structure of KK and its sediment cover. We have also used free-air gravity and magnetic anomaly data that supply important constraints on basement structure and its age of formation (Geological Survey of Japan 1996, 2000). Our main objectives are to document the tectonic history, structural characteristics and associated sedimentary facies of KK and to infer how the variations in sediment type and thickness around the knoll might modify the accretionary prism when it is subducted in the next million years or so.

GEOLOGICAL SETTING

The Nankai Trough is the convergent boundary between the subducting PSP and the overriding Eurasian Plate (Fig. 1a). The subduction rate varies along the Nankai Trough, from about 5 cm/year in the western part of the study area (52°W) to about 4 cm/year in the east (48°W; Seno *et al.* 1993). Changes in volcanic activity in western
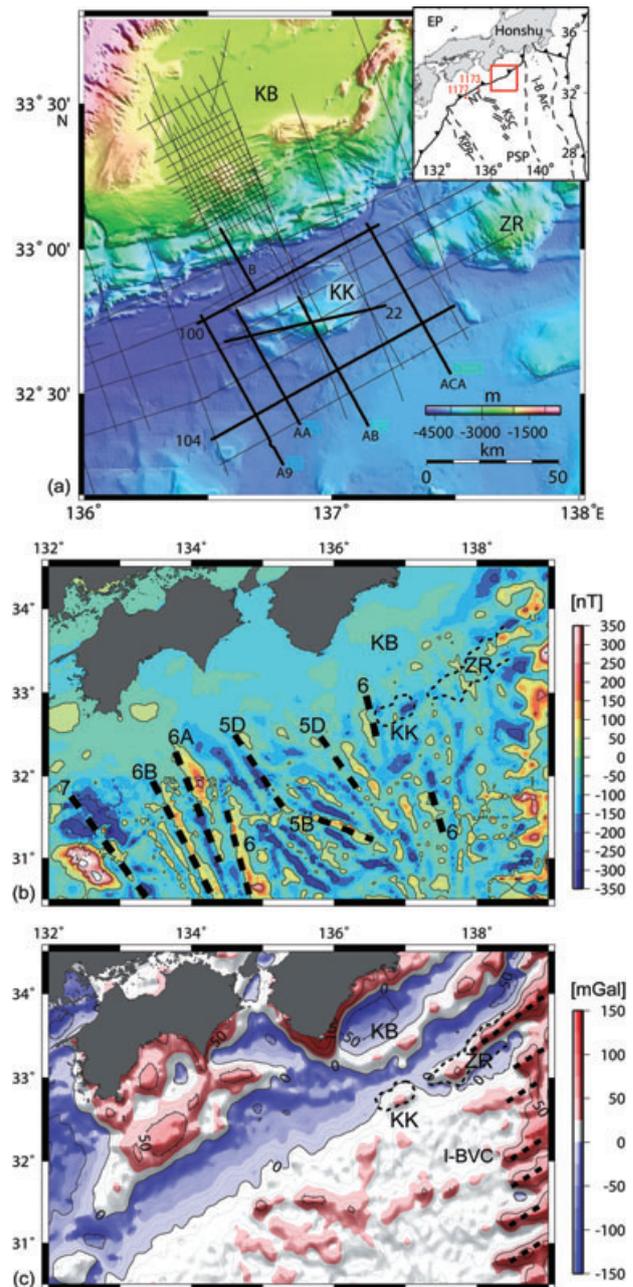
Fig. 1   (a) Regional bathymetric map showing locations of seismic lines used in this study. Solid bold lines are the track of the seismic lines presented in Figures 4–8. Line B was used to develop a velocity model. Insert box shows the tectonic map of the Philippine Sea Plate (PSP). EP: Eurasian Plate, I–B Arc: Izu–Bonin Arc, KB: Kumano Basin, KK: Kashinosaki Knoll, KSC: Kinan Seamount Chain, KPR: Kyushu–Palau Ridge, NT: Nankai Trough, ZR: Zenisu Ridge. Red circles show the location of ODP Sites 1173 and 1177. (b) Magnetic anomaly map of the northern Shikoku Basin (Geological Survey of Japan, 1996). Thick dashed lines represent the lineation of the major anomalies. Thin dotted lines indicate the outlines of KK and Zenisu Ridge. (c) Free-air gravity anomaly map of the northern Shikoku Basin based on compiled marine gravity data (Geological Survey of Japan, 2000). Thick solid lines are contours with 50 mGal intervals.

Japan have been used to suggest that subduction was very slow (<1 cm/yr) during 12–4 Ma, and increased to about 4–5 cm/year since about 4 Ma (Taira 2001; Kimura *et al.* 2005). Large amounts of terrigenous sediments are presently being channeled down the trench axis from the Izu–Bonin collision zone along the Suruga Trough into the Nankai Trough (De Rosa *et al.* 1986; Taira & Niitsuma 1986; Aoike 1999).

The basement structure of the Shikoku Basin, the northern part of the PSP, was formed by complex back-arc spreading in the Izu–Bonin island arc (Kobayashi & Nakada 1978; Nakamura *et al.* 1984; Hibbard & Karig 1990; Okino *et al.* 1994). Major spreading stopped around 15 Ma (Okino *et al.* 1994, 1999), but late-stage rifting may have continued until 7–10 Ma with associated volcanism that formed the KSC (Chamot-Rooke *et al.* 1987; Ishii *et al.* 2000).

Magnetic anomalies in the northern Shikoku Basin trend dominantly N–NNW (Fig. 1b), reflecting the seafloor spreading history (Kobayashi *et al.* 1995). Lineated magnetic anomalies in the western half of the Shikoku Basin clearly correlate with magnetic anomalies 6 to 7, but the anomalies in the eastern basin are less distinct and their correlations are less certain (Okino *et al.* 1999), possibly due to overprinting of the anomalies by arc-related volcanism (Taylor *et al.* 1992). An axial zone of NW-trending magnetic anomaly 5B–5D (Fig. 1b) reflects the late Miocene reorientation of the back-arc spreading center (Okino *et al.* 1994).

The free-air gravity anomalies generally trend parallel to the trench (Fig. 1c). Positive anomalies are centered over the SW Japan arc and the forearc ridge, whereas negative anomalies are centered along the forearc basin and the trench. The free-air anomalies seaward of the Nankai Trough are generally low (Fig. 1c), with the exception of positive anomalies over bathymetric highs such as KK, ZR, and NE-trending volcanic cross-chains of the Izu–Bonin arc system (Kaizuka 1975). We note that a negative gravity anomaly separates KK from ZR (Fig. 1c).

DATA ACQUISITION AND PROCESSING

SEISMIC REFLECTION DATA

We used three multi-channel seismic reflection data sets (Ike *et al.* 2008, Table 1) collected by the Japan Agency for Marine-Earth Science and Technology (JAMSTEC) over the eastern Nankai Trough and the NE Shikoku Basin. The first data set was collected from 1997 to 2001 on R/V *Kairei* using a variety of sound sources and multi-channel streamers. For data acquisition during the 1997 cruises, an air-gun array of 50 L (3080 in^3) was used as the sound source and a 120-channel streamer (25 m group interval) was used as the receiver. During the 2001 cruises, a 160-channel steamer and an untuned 196 L (~12 000 in^3) air-gun array was used as the sound source. Initial

Table 1 Seismic reflection data acquisition and processing parameters (Ike *et al.* 2008)

Acquisition parameters			
Survey initial	ODKM	ODKM	KR
Survey vessel	R/V *Kaiyo*	M/V *Polar Princess*	R/V *Kairei*
Recording year	2003–2004	2003	1997–2001
Seismic source	One GI gun	Tuned air-gun array	Non-tuned air-gun array
Gun volume (L)	5.7	70	~196
Shot interval (m)	25	50	50
Number of channels	18	480	160
Channel interval (m)	25	12.5	25
Processing sequence			
1.	Bandpass Filter (12–24–100–150 Hz)	Spiking Deconvolution	Bandpass Filter (3–5–100–120 Hz)
2.	Spiking/Predictive deconvolution	Bandpass Filter (8–12–72–80 Hz)	Deconvolution
3.	Spike & Noise Edit	Velocity analysis	Velocity analysis
4.	Velocity analysis	Dip moveout correction (DMO)	Normal moveout correction (NMO)
5.	NMO	NMO	Mute
6.	Mute	Mute	Stack (by JAMSTEC)
7.	Stack	Stack	F-K time migration
8.	F-K time migration	F-K time migration	Depth conversion
9.	Depth conversion	Depth conversion	

processing through stack for these lines was completed by JAMSTEC. We applied a second phase of advanced processing, including post-stack time migration and depth conversion. The second data set was collected by a commercial contractor in the spring of 2003 using a 480-channel steamer and a tuned 70 L (4240 in^3) air-gun array as the sound source (Taira *et al.* 2005). We processed several of these lines through stack and post-stack time migration, and performed pre-stack depth migration (PSDM) on lines ODKM-22 and ODKM-B. The third data set was collected on the R/V *Kaiyo* in December 2003–January 2004 using an 18-channel streamer and a single 5 L (355 in^3) generator-injector (GI) gun as the sound source. We have also processed these lines through stack and post-stack time migration. The relative resolution of the data sets is determined by the size and tuning characteristics of the air-gun arrays. Thus, data set one has the least resolution, but greatest depth of penetration due to its relatively low frequency content, data set two has higher resolution and data set three, having been shot with the highest frequency source, has the highest resolution, but the least depth of penetration.

We developed a velocity model based on the PSDM velocity field from ODKM-22 and ODKM-B and used these velocities for depth conversion of the other seismic lines. In areas where topography is relatively flat, we used a sediment velocity model of 1510 m/sec at the sea floor with a gradient of 0.65 km/sec^2 with increasing two-way travel time. We used a lower velocity gradient over KK (0.55 km/sec^2).

BATHYMETRY DATA

Multibeam bathymetry data were collected with the SeaBeam 2112 systems on the JAMSTEC vessels R/V *Kairei* and R/V *Yokosuka* during several expeditions (Fig. 2a). Post-processing consisted of editing the cross-track, navigation data and gridding using the MB-System software (Caress & Chayes 1996). The data were gridded with 100×100 m grid size and were merged with the regional satellite bathymetry data set of Sandwell and Smith (1997). We used the GMT function called 'grdgradient' to emphasize the knoll's slope structures (Wessel & Smith 1995). This function outputs the scalar magnitude of gradient vectors for each slope obtained from bathymetric data. Subsequently, we converted the outputs of slope angle from radians to degrees and then used 'grdimage' to create a color-coded image of the
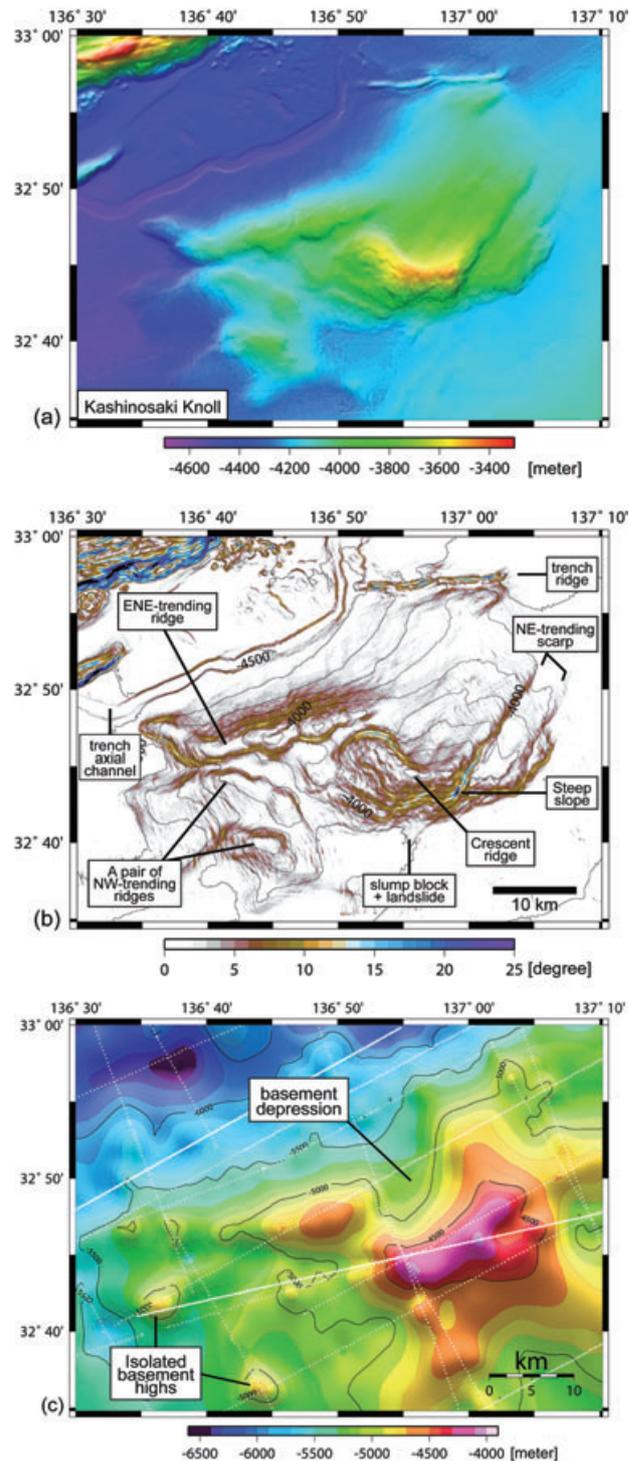
Fig. 2 (a) Bathymetric map of Kashinosaki Knoll. A depth color scale is shown. (b) Slope angle map with interpretation of the sea floor morphology. Solid lines are the bathymetric contours with 100 m intervals. A color scale for each angle is shown. (c) Basement topography map. Thick solid lines are topographic contours with 500 m intervals. White dots are sampling points for the basement depths.

slope angle along with the bathymetric contours (Fig. 2b).

SEISMIC STRATIGRAPHY

Seismic stratigraphic sequences, defined in the western and central Nankai Trough off Shikoku Island, have been sampled by ocean drilling (Karig *et al.* 1975; Taira *et al.* 1991; Moore *et al.* 2001). There are three major seismic stratigraphic sequences above the acoustic basement (Fig. 3): (i) lower Shikoku Basin (LSB) sequence; (ii) upper Shikoku Basin (USB) sequence; and (iii) Quaternary turbidite sequences. These sequences are correlated with the key lithostratigraphic units defined at the ODP Legs 131 and 190 drill sites (Fig. 3). Seismic line ODKM-102 crosses over ODP Site 1173 and runs parallel to the Nankai Trough axis, allowing us to extrapolate the seismic sequences defined at the drill site into our study area south of the Kumano Basin (Ike *et al.* 2008).

The oldest unit, the LSB sequence, overlies a thin drape of volcaniclastic sediments above the basement. It is characterized by low amplitude reflections in the lower section, and relatively high amplitude, discontinuous to moderately-continuous hummocky reflections at its upper boundary (Fig. 3). This sequence is correlated with the middle Miocene to lower Pliocene hemipelagic mudstones sampled at the ODP drill sites. We interpret high amplitude, laterally continuous reflections within the LSB sequence in the western Shikoku Basin as a subunit (LSB-T) that correlates with turbidite sands recovered at ODP Site 1177 (Moore *et al.* 2001; Ike *et al.* 2008). The probable source of these turbidites is suggested to be south-western Japan, the inner zone of Shikoku Island, with delivery of sediment across the trench and out onto the Shikoku Basin floor (Fergusson 2003).

The second sequence, the USB sequence is characterized by low-amplitude, moderately-continuous reflections in the seismic data. This sequence was originally defined by an abundance of ash layers in the ODP cores (Taira *et al.* 1991; Moore *et al.* 2001). Furthermore, its lower boundary is controlled in part by the diagenetic breakdown of ash layers in the lower unit.

The third and youngest seismic sequence, another turbidite unit, exhibits laterally continuous and high amplitude reflections that lap onto the USB sequence. It is correlated with the 'trench facies' at the ODP sites, although the distribution of Quaternary turbidites in our study area is not restricted to the morphologic trench.

STRUCTURAL CHARACTER OF KASHINOSAKI KNOLL

OCEAN FLOOR MORPHOLOGY

Kashinosaki Knoll is approximately 30×40 km, forming a rectangular body that is elongated to the ENE (Fig. 2a). The knoll is bathymetrically separated from ZR by a 25 km wide flat plain (Fig. 1a). The knoll's summit, approximately 40 km south from the trench landward slope, is characterized by four ridges separated by narrow valleys: (i) an
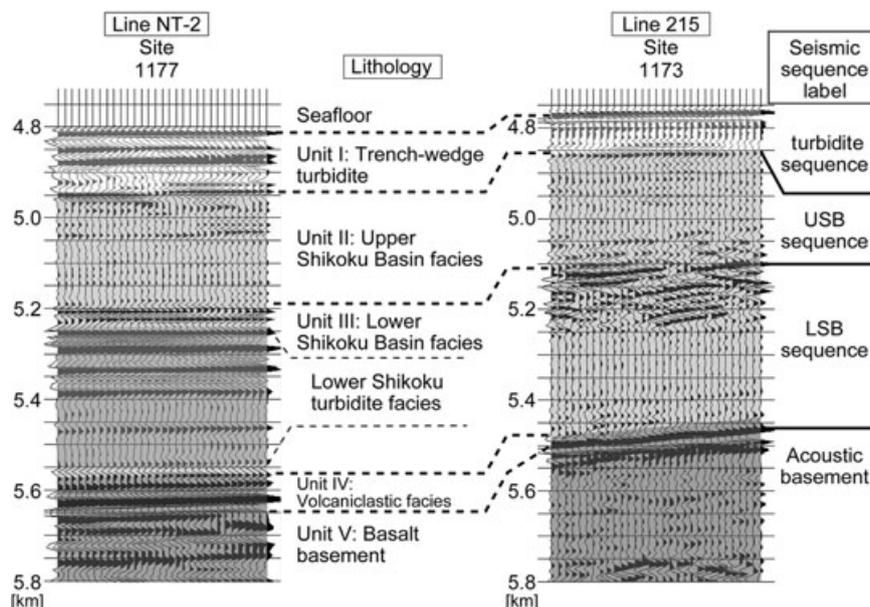
Fig. 3 Depth-converted seismic reflection data showing the seismic stratigraphy of the Shikoku Basin sediments correlated with ODP sites 1173 and 1177. Seismic line NT-2 with ODP site 1177 is on the left, and line 215 with site 1173 is on the right (Moore *et al.* 2001). Vertical axis is depth in meters.

ENE-trending ridge located on the northwest side of the knoll, with depth ranging from 3.9 to 4.5 km; (ii) a pair of NW-trending ridges on the southwest side, with depth ranging from 4.0 to 4.5 km; and (iii) a crescent-shaped ridge, forming the summit of KK that is about 600 m higher than the adjacent flat seafloor (Fig. 2b). Each ridge is undissected and lacks volcanic morphologies such as craters or cones.

The gentle north-dipping bathymetric slope on the eastern side of the crescent ridge is cut by two major NE-trending scarps. The southern slope of the crescent-shaped ridge has a steep landslide scarp that dips about 10–20° south, and has a slump block at its flank. The NW-trending ridges have smooth western slopes of about 7°. The northern slope of KK is about 12° on the western half along the ENE-trending ridge, and about 3° on the eastern half. North of KK, there is a narrow ridge about 18 km long, about 1 km wide and about 50 m high, located at the edge of the trench. It trends roughly east-west, and its western edge terminates near the trench axial channel.

FREE-AIR GRAVITY AND MAGNETIC ANOMALIES

Magnetic anomalies trend NNW–SSE across the western flank of KK, and magnetic anomaly 6 (19–20.5 Ma) is parallel to the knoll just to the west (Kido & Fujiwara 2004) (Fig. 1b). Over the summit, there is a dipolar anomaly that is positive (~100 nT) on the SW and negative (~–200 nT) on the NE (Fig. 1b). The orientation and intensity of the magnetic anomaly on the knoll are distinct from that observed over ZR. The positive amplitude of the anomaly over ZR is more than about 50 nT higher than over KK. Along ZR, the trend of magnetic anomalies is dominantly NE–SW, with positive on the SSE and negative on the NNW. The anomalies extend to the SW, likely overprinting the anomalies related to the back-arc spreading of the northern Shikoku Basin (Chamot-Rooke *et al.* 1987; Taylor *et al.* 1992). Seafloor spreading magnetic anomalies indicate that the crustal age across the south part of ZR is 22 to 24 Ma (anomalies 6B and 6C) (Lallemant *et al.* 1989). We interpret magnetic anomaly 6A (20.55 Ma) crossing the Kashinosaki Knoll (B. Taylor, pers. comm., 2006).

The free-air gravity anomalies also highlight differences between KK and ZR (Fig. 1c). Although there are positive anomalies over both KK and ZR, the two features are separated by an area of negative anomaly. The positive anomaly over KK is circular, while the anomaly over ZR is elongated

and continuous to the NE, and the anomaly over KK is 30–80 mGal lower than the anomaly over ZR. There is a distinct negative anomaly south of ZR, but a similar negative anomaly is not present south of KK.

BASEMENT STRUCTURE OF KASHINOSAKI KNOLL AND ITS SURROUNDINGS

Seismic profiles reveal that the basement summit of KK does not directly underlie the seafloor summit (Figs 2c,4). At the sea floor summit of KK's Crescent Ridge, there is a basement peak that is 4 km below sea level, but the basement summit is approximately 8 km to the east from the knoll's bathymetric peak (Figs 4,5). Between these two basement peaks toward the northern slope of KK, there is a NS-trending basement depression that is not present in the bathymetry. The maximum depth of this depression is about 250–300 m near the summit of KK, and it decreases to the north. The basement slope landward of KK is about 5–15°, while the seaward slope of the knoll is about 20–30° (Fig. 5).

At a local scale, there are two isolated basement highs (IBH) with little or no bathymetric expression, one on the western flank of KK (Figs 2c,4), and another on the southwestern flank (Figs 2c,6). These basement highs have three characteristics in common: (i) a diameter that is approximately 5 km at their base; (ii) a peak about 600 m higher than the adjacent basement; and (iii) a basement slope up to 20°. The overlying sediment thickness ranges from about 200–400 m over the peaks, and increases away from the peaks. We note that the IBHs are too small to overprint the NS-trending magnetic anomalies that cross KK.

In other parts of KK, there are basement structures that are present in the bathymetric trends. The basement structure on the eastern side of KK is generally parallel to the bathymetry except over the two NE-trending scarps (Fig. 4, shot point [S.P.] 1860, 2000). For instance, over the basement summit, the total sediment thickness decreases from about 550 m near the bathymetric summit of KK to about 200 m above the basement summit (Fig. 4, S.P. 1860). To the east of KK, the sediment thickness between S.P. 1860 and S.P. 2000 is about 500 m, and it decreases to about 200 m at the scarp. To the west from the summit of KK, the basement structure beneath the pair of NW-trending ridges is relatively planar, with an approximately 5° slope that generally dips to the west (Fig. 2c).
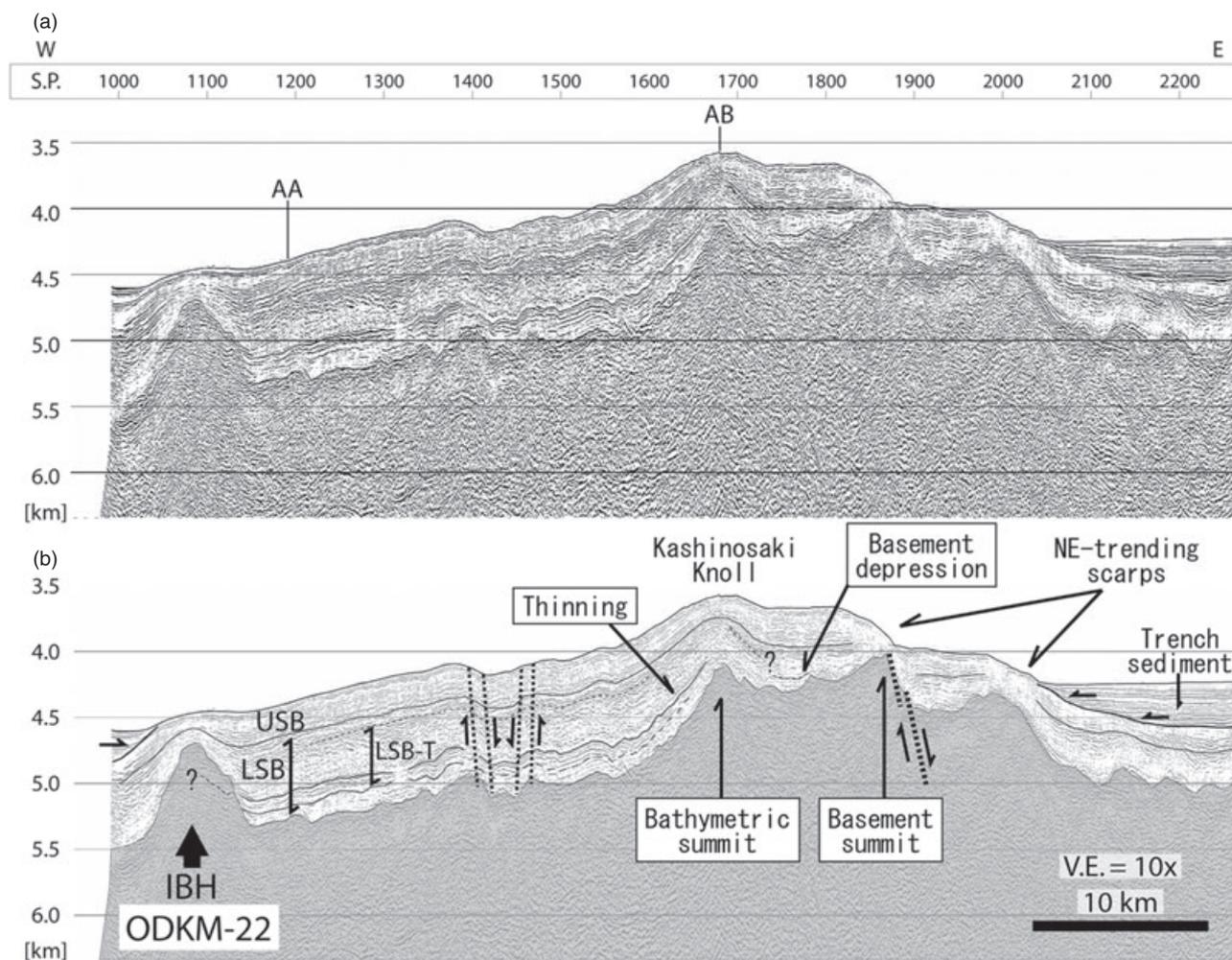
Fig. 4 Seismic depth section ODKM-22 crossing over the summit of Kashinosaki Knoll, oriented approximately parallel to the trench axis. The location is shown on Figure 1. S.P. = shot point, shot interval = 50 m. (a) Uninterpreted section. Cross lines are labeled with a vertical line and a line number. (b) Interpreted section. Thick dotted lines represent faults. Thick solid line represents the bottom of the Quaternary turbidite. IBH: Isolated Basement High. LSB: lower Shikoku Basin sequence, USB: upper Shikoku Basin sequence. In both sections, vertical axis distances are in kilometers. Vertical exaggeration (V.E.) is 10×.

Basement relief around KK is also very complicated. The basement highs trend roughly perpendicular to the trench; seismic lines parallel to the trench axis show long-wavelength and high-amplitude basement features (Fig. 7), whereas lines perpendicular to the trench do not show high-amplitude basement relief (Fig. 8). The amplitude of the short-wavelength basement relief parallel to the trench between KK and the trench is 200 m to the northwest of KK, and increases to 500 m northeast of the knoll (Fig. 7).

Along the west side of KK, there are several short-wavelength and low-amplitude basement highs (Fig. 8). The basement relief in this area is generally subdued compared with other areas. The basement relief on the south side of KK has a wavelength of about 25–30 km (Fig. 9). The amplitude of the basement relief (~500 m) in this area is similar to that north of the knoll.

The trench-perpendicular line shows undulation in the basement relief between KK and ZR. The relief is lineated parallel to the trench axis with a wavelength of about 5 km and amplitude of about 400 m on the northern half, and a wavelength of about 10 km and amplitude of about 250 m on the southern half (Fig. 10).

SEDIMENTATION PATTERNS OVER AND AROUND KASHINOSAKI KNOLL

Our seismic profiles clearly image variations in sediment thickness and type that are controlled by the basement structure of KK (Fig. 11). The total sediment thickness around KK ranges from about

(a)

(b)
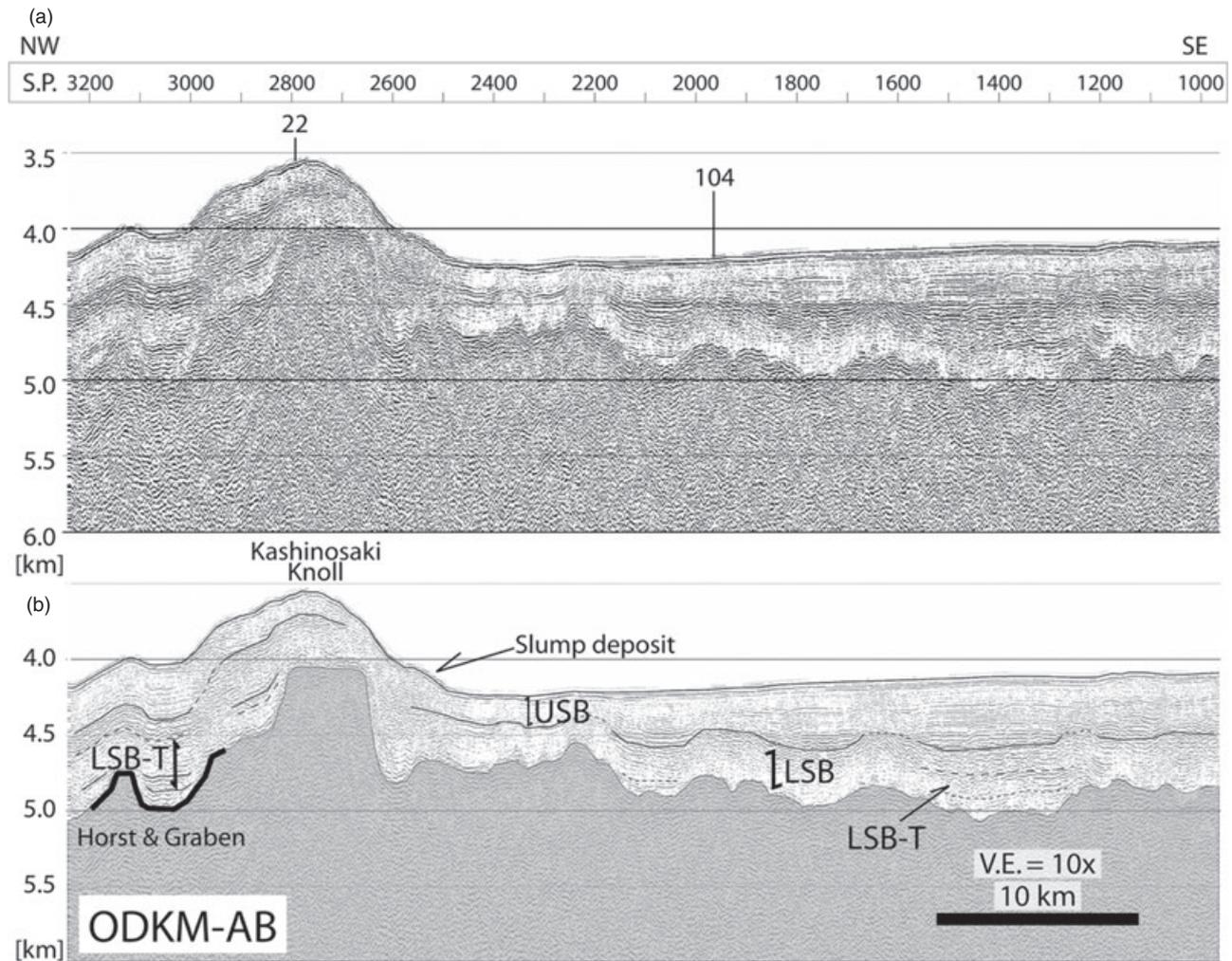
Fig. 5   Seismic depth section ODKM-AB crossing over the summit of Kashinosaki Knoll, oriented perpendicular to the trench axis. S.P. = shot point, shot interval = 25 m. Vertical exaggeration (V.E.) is 10×. (a) Uninterpreted section, (b) interpreted section.

300 to 1600 m. The maximum thickness occurs along the trench axis and between KK and ZR (Fig. 10). The minimum thickness, less than 300 m, occurs over the basement summit of KK (Fig. 4). Within our study area, the average total sediment thickness over KK is approximately 40–50% more on the western and northern slopes than that at the summit, southeastern slopes, and over IBHs where the basement slope is steep (~20°) (Fig. 11). At a local scale, the total sediment thickness along the western slope of KK ranges from 850 to 1000 m, and is nearly constant along the gentle basement slope and to the west (Figs 4,6). Northwest of KK, the graben along the NW-trending ridge has 15–20% more sediments than the adjacent horst (Fig. 6). At the summit of KK, the total sediment thickness is approximately 590 m and it decreases toward the eastern slope. To the south, the south-ern flank of KK has sediment thickness similar to that over the summit (Fig. 5). Sediment thickness increases in parallel with the increase of the base-ment depth to the south (Figs 5,9). In this area, the reflections within each seismic sequence show similar patterns with the west side of KK, such as the continuous and discontinuous reflections within the LSB-T subunit (Fig. 5, S.P. 1210–1650).

LSB sequence

The upper boundary of the LSB sequence varies locally in depth, with depth variation being posi-tively correlated with sea floor depth: the LSB sequence is thicker in the basement lows than over the basement highs. The thickness of the LSB sequence is roughly 60% of the total sediment thickness, except in local areas where the LSB-T
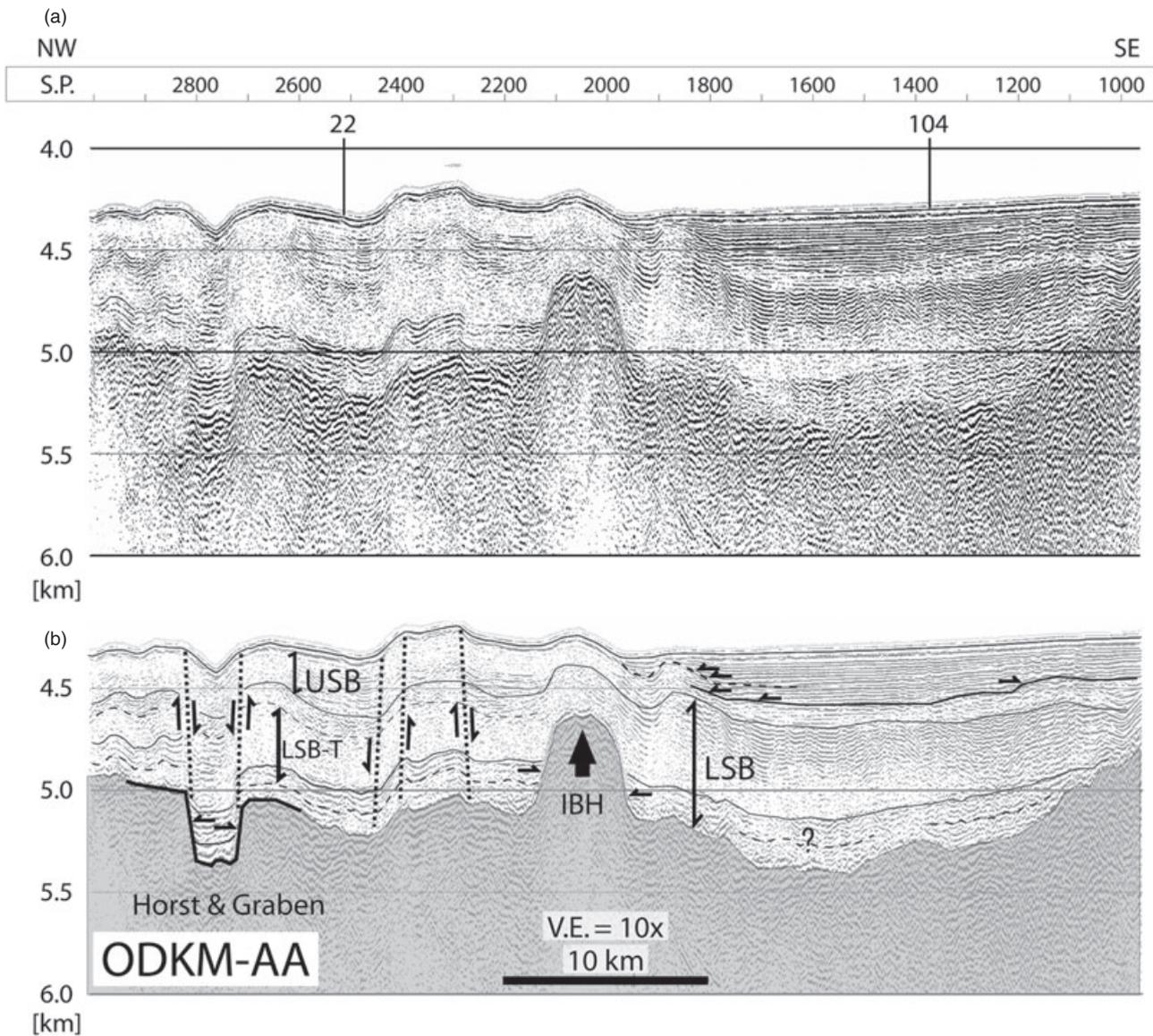
Fig. 6 Seismic depth section ODKM-AA over the western side of KK, perpendicular to the trench axis. Axes are the same as Figure 5. (a) Uninterpreted section, (b) interpreted section.

subunit is absent, and in areas where Quaternary turbidites are deposited. The thickness of the LSB sequence is more than 500–600 m where the LSB-T subunit appears in the sediment sequence, whereas it is less than about 400 m where the LSB-T subunit is absent or poorly defined. In detail, the thickness of the LSB sequence is approximately 350 m at the bathymetric summit of KK, and it is less than 200 m over its basement summit to the east (Fig. 4). To the southwest, over the pair of NW-trending ridges, its thickness is approximately 500 m except for the areas over IBH where its thickness is less than about 250 m (Fig. 6). To the northwest, over the ENE-trending

ridge, its thickness is about 600 m over the horst and 800–850 m within the graben (Figs 5,6).

LSB-T subunit

The distribution of the LSB-T subunit is controlled by the topography of KK (Fig. 11). LSB-T clearly appears along the northern slopes of KK including the ENE-trending ridge located on the north-west flank (Fig. 5). There is generally a section (~100 m) of low amplitude reflections, underneath LSB-T, that drapes over the basement (Figs 4,5), but this subunit is locally absent over steep basement slopes. The thickness of the LSB-T subunit
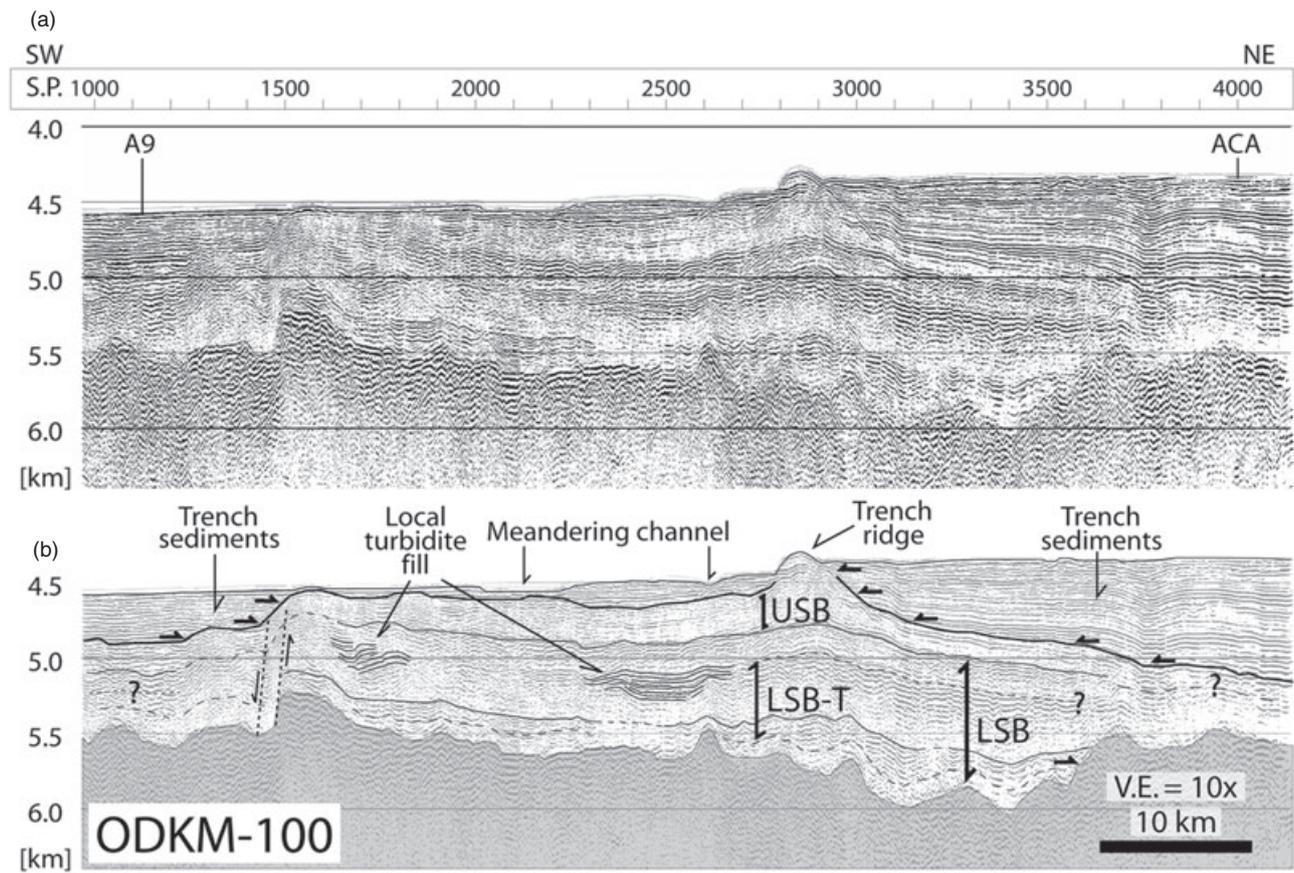
Fig. 7 Seismic depth section ODKM-100 over the northwestern end of KK, parallel to the trench. Axes are the same as Figure 5. (a) Uninterpreted section, (b) interpreted section.

ranges from 100 to 500 m, but locally is either less than 50 m, or absent, over basement highs. To the southwest, at the pair of NW-trending ridges, the upper boundary of LSB-T is sub-parallel to the underlying basement (Fig. 4). This subunit is characterized by thinning toward the summit of KK. The LSB-T subunit onlaps the basement around the IBHs on KK's flanks, but generally is parallel to basement slopes that are less than 5–10°, such as on the northwestern area of KK (Figs 4,6).

Reflection amplitude is relatively low and the internal structure is relatively horizontal on the eastern flank of KK where the slope is steep. On these steep slopes, the high amplitude reflections that characterize LSB-T are either poorly defined or absent (Fig. 4a, S.P. 2000–2050). Similar relationships between the basement structure and the seismic character of LSB-T occur on the southern slope of KK where the steepest (~20°) basement slope correlates with the steep bathymetric slope (Figs 2b,5). The LSB-T subunit is also absent near the southern flank of KK.

Away from KK, the LSB-T subunit laps onto basement highs and fills basement lows (Fig. 7, S.P. 2600–3600). To the west, it has low amplitude discontinuous reflections (Fig. 7, S.P. 2300–2600). Within the LSB sequence in this area, but above LSB-T, there are high amplitude reflections suggestive of a channel and levee structure. This channel and levee structure also occurs near the relative basement high to the west in a similar depth (Fig. 7, S.P. 1600–1800). On the northwestern side of KK, reflections in the LSB-T subunit are parallel to the local basement high and become unclear to the west underneath the trench sediments (Fig. 7, S.P. 1000–2200). There is a section (~100 m) of low-amplitude reflections in between the LSB-T subunit and the basement (Fig. 7).

On the southwestern side of KK, the LSB-T subunit has high amplitude reflections in the upper half of the unit, although the reflection amplitudes decrease in the lower half. It is parallel to the basement, but locally laps onto IBHs (Fig. 8, S.P. 2520–3300). To the south, LSB-T
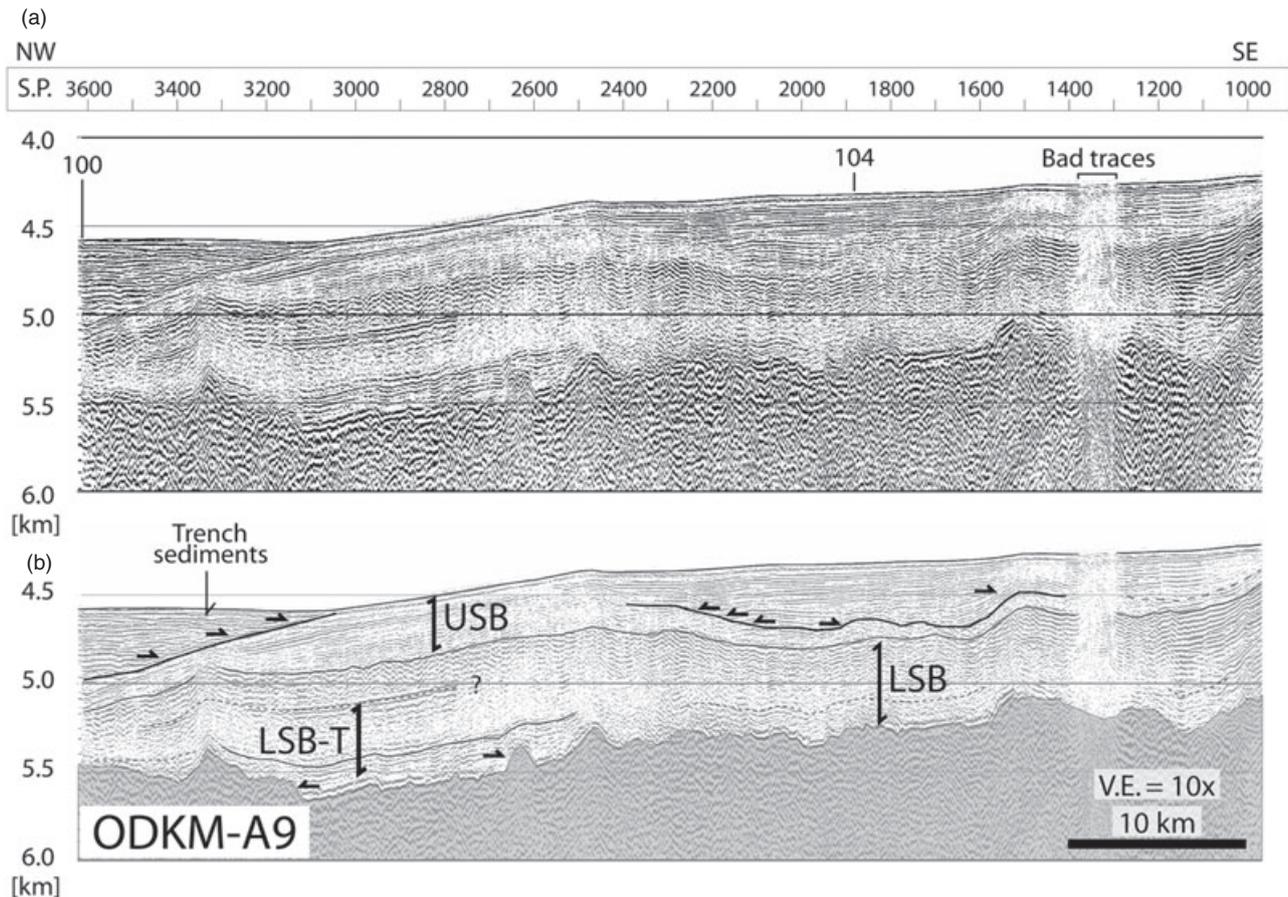
Fig. 8 Seismic depth section ODKM-A9 over the western end of KK, perpendicular to the trench axis. Axes are the same as Figure 5. (a) Uninterpreted section, (b) interpreted section.

shows discontinuous low-amplitude reflections over basement (Fig. 8, S.P. 1000–2500). The low-amplitude reflections within LSB-T clearly appear on the trench-parallel seismic cross-line ODKM-104 (Fig. 9).

The LSB-T subunit clearly appears in basement lows on the southwest side of KK, but it is poorly defined over the basement highs to the east. The thickness of LSB-T on the southwest side of KK is about 200 m and is roughly constant over the basement relief, similar to the northwestern slopes of the knoll. The thickness of LSB-T locally increases up to 400 m between S.P. 2300 and S.P. 2600, but the overall regional trend is eastward thinning (Fig. 9). The thinning is similar to the western (Fig. 4a, S.P. 1500–1650) and northeastern (Fig. 7, S.P. 3400–3600) slopes of KK in terms of its deposition against basement highs. To the east, over the relative basement high between S.P. 2800 and S.P. 3900, the LSB-T subunit is characterized by low amplitude discontinuous reflections, and its thickness is less than 100 m, similar to its character at

the summit of KK (Fig. 9). The subunit is poorly defined or absent from S.P. 3900 to S.P. 4600, similar to areas along the eastern slope of KK.

USB sequence

The USB sequence clearly appears over and around KK (Figs 5–10). The internal reflections in the USB sequence are parallel to the upper boundary of the LSB sequence; however, they show subparallel, low-amplitude reflections over IBHs. Around KK, the seismic character of USB shows relatively subdued and lower-amplitude reflections compared with the upper boundary of the LSB sequence. The upper portion of the USB sequence has low-amplitude reflections where they are not overlain by the Quaternary turbidites. The thickness variation in the USB sequence is roughly up to 40% of the total sediment thickness over KK (100–350 m). This trend holds on the northern and western slopes of KK; however, it is disrupted where the USB sequence

(a)

(b)
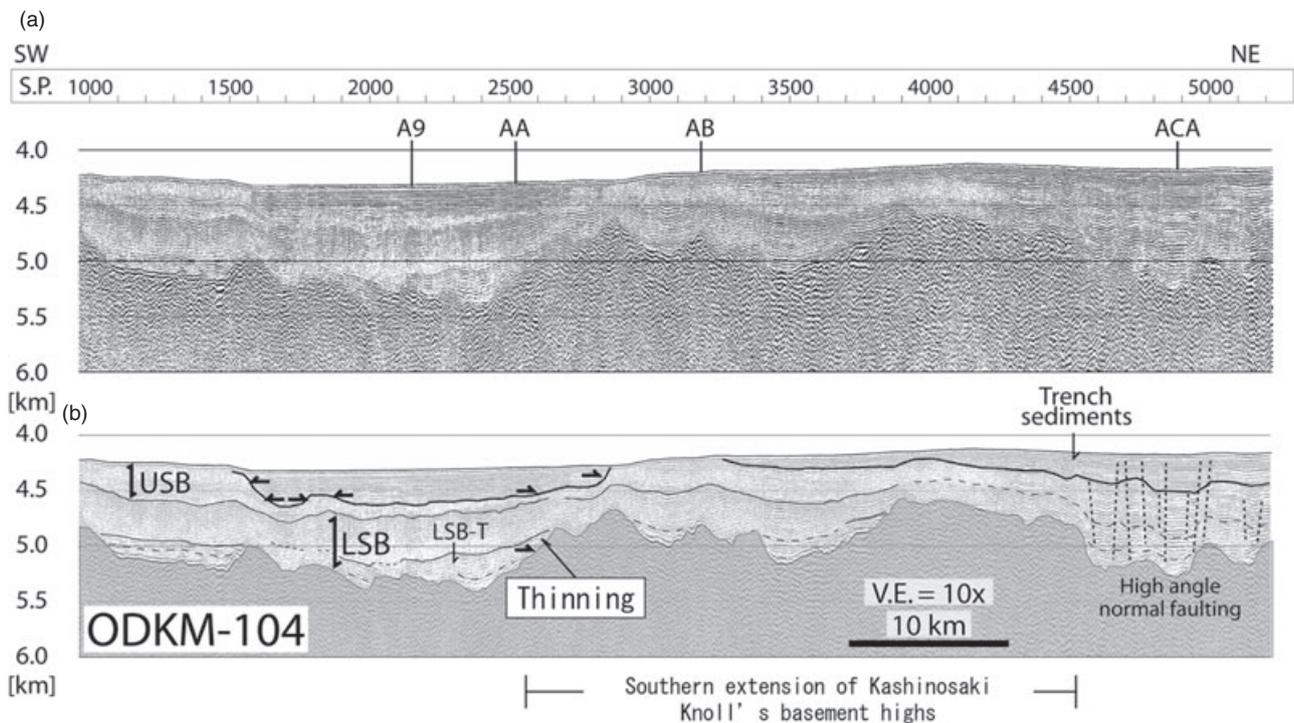
Fig. 9　Seismic depth section ODKM-104 over the south side of KK, parallel to the trench axis. Axes are the same as Figure 5. (a) Uninterpreted section, (b) interpreted section.

is overlain by the Quaternary trench turbidites or where the total sediment thickness is less than about 400 m, such as over the IBH and near the basement summit similar to the LSB sequence (Figs 4,6,7).

Quaternary turbidites

Quaternary turbidites overlie the USB sequence. The majority of the turbidites accumulate around the knoll, particularly along the trench, between KK and ZR, and partly on the southern and south-western regions of KK, where they fill topographic lows (Figs 7,9). The Quaternary turbidites are not deposited over KK (Fig. 4a).

Sediments between Kashinosaki Knoll and Zenisu Ridge

The seismic character of the LSB and USB sequences is different between KK and ZR than in other parts of the study area (Figs 9,10). The LSB sequence is dominated by low amplitude, discontinuous reflections that generally drape over basement highs. Some reflections within the LSB sequence may be the candidates for the LSB-T subunit; however, we find that LSB-T in this area is usually isolated to structural lows (Fig. 10, S.P. 1000–2600). For instance, on line ODKM-100 at about S.P. 4000, the LSB-T subunit is absent, whereas the subunit laps onto the basement high at about S.P. 3500 (Fig. 7). Overlying the LSB sequence, the USB sequence is characterized by high-amplitude continuous reflections that partially lap onto the upper boundary of the LSB sequence (Fig. 10, S.P. 2000–2350). The USB sequence in this area is characterized by high-amplitude continuous reflections that are distinct from other areas. We define the upper boundary of the USB sequence by an unconformity at the lower boundary of the trench wedge turbidites. The unconformity is difficult to distinguish from other reflections to the south, indicating that the young trench wedge sediments are transported not only along the trench but also out of the axial trench channel to the south, between KK and ZR, and on the southern side of KK. In addition, within this area, high angle normal faults displace all of the sediment sequences (Fig. 10). The dip angles of these faults range from 75 to 85° and offset the entire sediment column for 10–30 m. The geometry of these faults is not correlated with the basement relief. We do not find strong evidence for similar fault displacement on the west side of KK (Fig. 8).
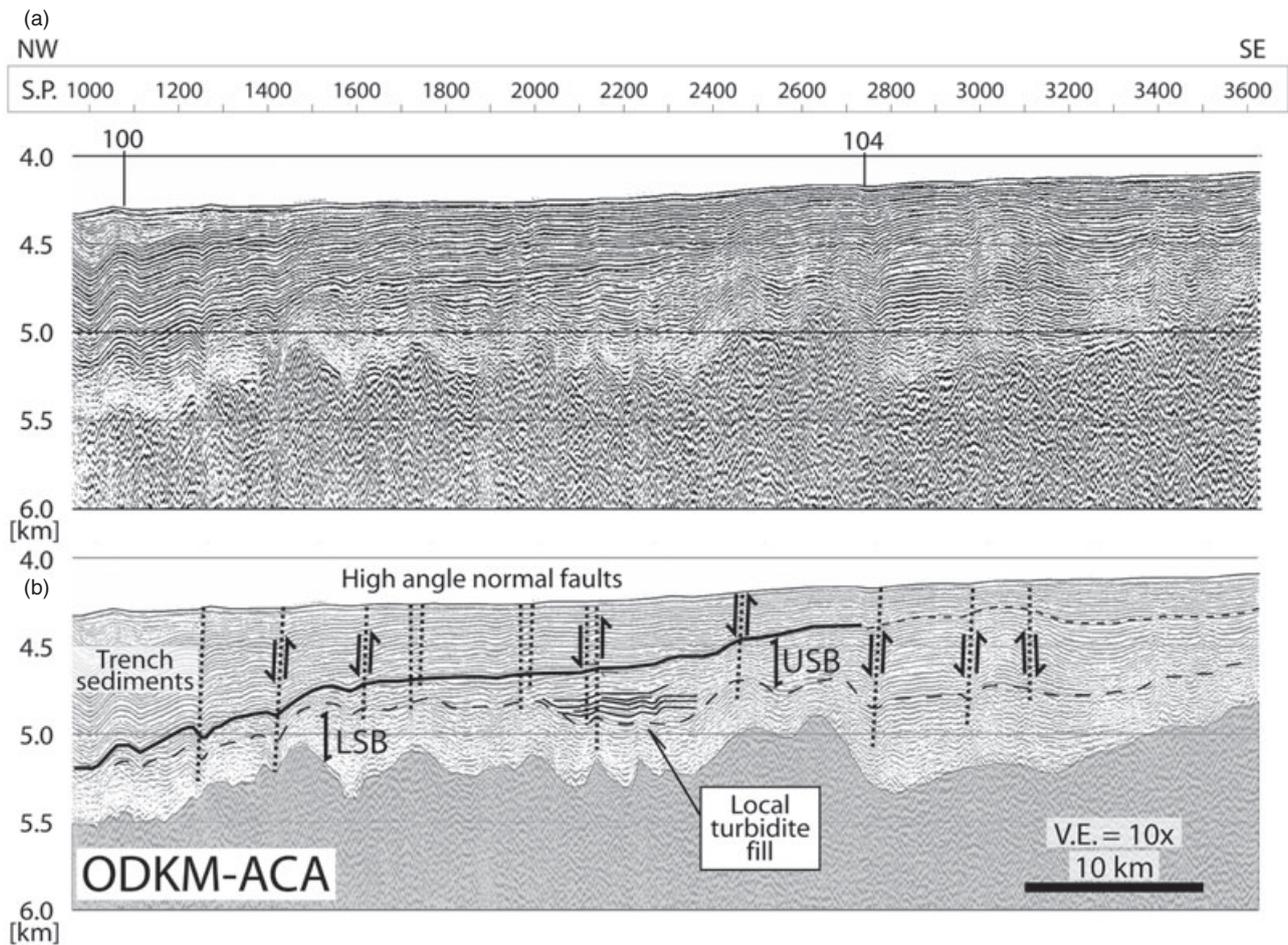
Fig. 10 Seismic depth section ODKM-ACA between KK and Zenisu Ridge, perpendicular to the trench axis. Axes are the same as Figure 5. (a) Uninterpreted section, (b) interpreted section.
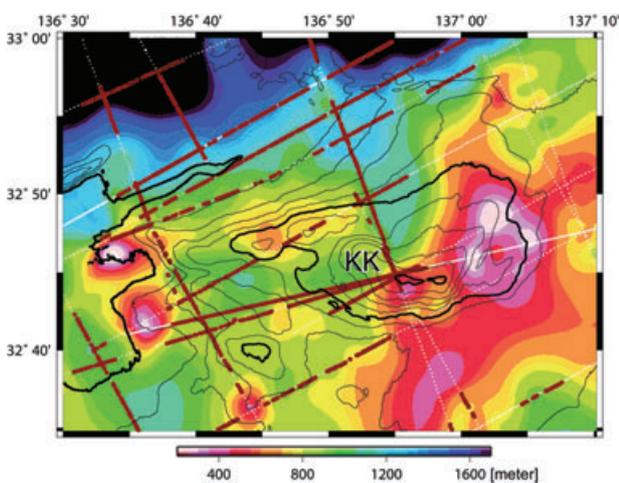
Fig. 11 Total sediment isopach map of KK. A color isopach scale is shown. Solid lines are bathymetric contours with 500 m (thick) and 100 m (thin) intervals. White dots are sampling points for the total sediment thickness. Red dots show the occurrence of the LSB-T subunit. KK: Kashinosaki Knoll.

DISCUSSION

THE ORIGIN OF KASHINOSAKI KNOLL

Our new bathymetric and seismic reflection data, coupled with existing gravity and magnetic anomaly data, provide insight into the origin of KK, and processes of sedimentation over and around this isolated topographic high in the eastern Nankai Trough. Several interrelated processes are responsible for shaping the knoll's tectonic and sedimentary evolution: its formation about 700 km south of its current location, variations in sedimentation patterns and processes caused by the knoll itself, and late stage normal faulting associated with basement deformation.

It has been proposed that KK is the westward extension of ZR and that the north-dipping thrust fault underlying ZR continues westward under KK (e.g. Le Pichon *et al.* 1987; Lallemant *et al.* 1989). We noted above, however, that there are

striking differences in the magnetic and gravity anomalies over KK and ZR, and the anomalies between the two areas are not continuous. Furthermore, our seismic reflection data show that the basin between ZR and KK is filled with undeformed sediments, further indicating that the thrust under ZR does not extend westward. These observations strongly suggest that the two features have different geological origins (Fig. 1b,c). ZR was likely formed by thrust faulting related to the Izu–Bonin collision to the east (Le Pichon *et al.* 1987), whereas KK appears to be an isolated feature.

The high amplitude dipolar magnetic anomaly pattern observed over is more suggestive of an isolated volcanic feature (Parker 1991). The seismic reflection data do not support the existence of the thrust faults south of KK inferred by Le Pichon *et al.* (1987). We thus favor a volcanic origin for KK. Such isolated volcanic highs are common throughout the northeastern Shikoku Basin (Fig. 1a,b).

The lowest sedimentary unit (LSB-T subunit) onlaps the basement flank of KK, indicating that the knoll was already in place before LSB-T sedimentation began. Therefore, KK must have been formed soon after the crust was formed by seafloor spreading in the middle Miocene (20–21 Ma). Given the age of the knoll and the estimated subduction rate (10 cm/yr during 17–12 Ma, 1 cm/yr during 12–4 Ma, 4 cm/yr during 4–0 Ma, Kimura *et al.* 2005), the knoll probably formed more than 700 km southeast of its present location and has been transported to the northwest by subduction of the Shikoku Basin beneath Japan (Fig. 12).

EXTENSIONAL DEFORMATION OVER KASHINOSAKI KNOLL

The bathymetry data show two NE-trending scarps on the southeastern slope of KK. The apparent offset of these scarps is 250–300 m. Seismic profiles crossing these scarps show normal faulting displacement of the basement with about 500 m offset (Fig. 4a, S.P. 1880, 2050). The sediment layers between the two bathymetric scarps are nearly horizontal. To the east, the sediment package between KK and ZR shows normal faults that appear to cut through most of the deep as well as shallow sediments (Figs 9,10). Normal faults and large scale slumping are common on the flanks of most oceanic seamounts (e.g. Mitchell 2003; Morgan *et al.* 2003; Kerr *et al.* 2005). Given the proximity of KK to the trench outer slope, it is likely
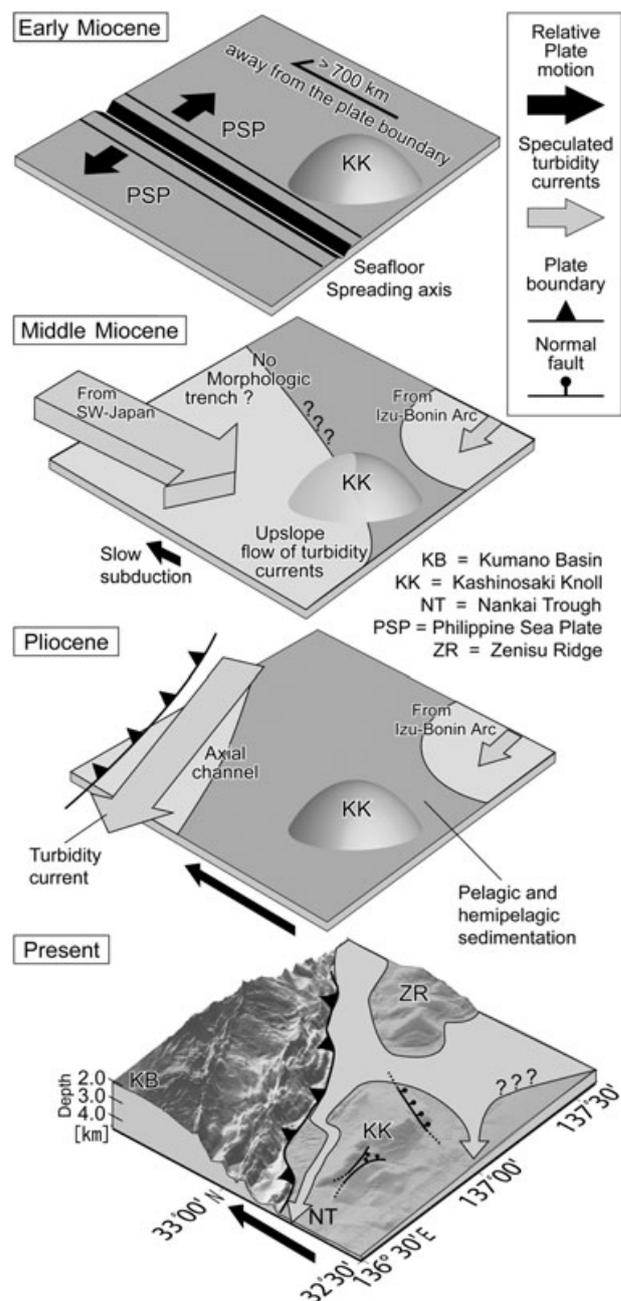
Fig. 12 Diagram showing the tectonic development of KK since the early Miocene. Light gray arrows show the direction of turbidity current transport around KK. Gray colors represent pelagic and hemipelagic sedimentation.

that the normal faulting was enhanced by bending stresses as the knoll approached the trench, which further promoted slumping.

SEDIMENTATION OVER AND AROUND KASHINOSAKI KNOLL

The onlap of the LSB-T subunit onto IBHs and other relative basement highs indicates the base-

ment relief of KK was reached by Miocene turbidity currents coming from Japan (Figs 4,6,9,11). Turbidites from Shikoku are not currently able to reach very far out onto the Shikoku Basin because they are trapped in one of forearc basins, in small basins on the accretionary prism, or in the trench. Thus, the occurrence of the LSB-T subunit over the knoll suggests that the margin must have been very different in the Miocene, with no morphologic trench or forearc basins. The subduction of the young, warm Shikoku Basin lithosphere probably precluded formation of a deep morphologic trench (similar to the current situation off Cascadia). In addition, we suggest that the extremely low subduction rate during this time (Kimura *et al.* 2005) would have led to very slow outbuilding of the accretionary prism, allowing submarine canyons to more easily cut across the inner trench slope and flow out onto the Shikoku Basin floor. The LSB-T subunit probably represents turbidites that flowed from Shikoku and western Honshu, and were channeled into topographic lows in the Shikoku Basin floor (Fergusson 2003). Infrequent higher-energy flows may have also climbed up the northwest-facing slope of KK (e.g. Muck & Underwood 1990; Ricci-Lucchi & Camerlenghi 1993).

Above the LSB-T subunit, high amplitude continuous reflections characteristic of turbidite deposits are absent in both the LSB and USB sequences north, south, and west of KK. This observation is consistent with the inference of rejuvenation of Philippine Sea subduction in the late Miocene (Kimura *et al.* 2005). Accelerated subduction would have led to formation of the trench and rapid outbuilding of the accretionary prism and formation of forearc basins that would have inhibited flow of turbidity currents from Japan out onto the Shikoku Basin floor, assuming that the rapid outbuilding of the accretionary prism outpaced erosion by submarine canyons, so that turbidites did not reach the floor of the Shikoku Basin, even though the KK region was being carried much closer to the margin.

In the region between KK and ZR, the USB sequence exhibits high-amplitude continuous reflections characteristic of turbidite deposition (Figs 9,10). We interpret the majority of these high-amplitude reflections observed between KK and ZR to be turbidites that were sourced from the Izu–Bonin arc to the east. They are restricted to the regional low southeast of KK because the volume of flows was not great enough to fill the basin and flow around KK.

Quaternary deposits that overlie the USB sequences in the Nankai Trough are dominated by thick turbidites sourced from the Izu collision zone to the NE (e.g. Taira & Niitsuma 1986; Fergusson 2003), and spill-over from the Tenryu Canyon that forms a canyon-mouth fan superimposed on the axial–channel system (Soh *et al.* 1991). North and west of KK, these deposits form a classic trench wedge (Figs 7,8), similar to the wedge off Shikoku (Moore *et al.* 2001). Similar deposits of thick Quaternary turbidites onlap the southern and eastern margins of KK (Figs 9,10) and also overlie the USB sequence east of KK (Figs 7,10). These observations suggest that KK's approach to the Nankai Trough partially dammed the path of Quaternary turbidity currents flowing along the trench axis, diverting part of the flow between KK and ZR onto the Shikoku Basin floor. The introduction of these topographic highs into the trench disrupts the normal flow of trench turbidites, and in turn leads to significant along-strike variations in sediment thickness and type entering the subduction zone.

Local variations in both sediment thickness and type are likely to strongly influence the styles of deformation within the accretionary prism, likely leading to rapid along-strike variations in thickness, width and composition of individual accreted thrust packages.

CONCLUSIONS

Analysis of regional seismic stratigraphic, magnetic, and gravity data provide insight into the origin of Kashinosaki Knoll and its control on sedimentation in the eastern Nankai Trough. KK is a relatively old volcanic feature of the Shikoku Basin that was formed soon after the crust was generated well south of its present location in the early Miocene (Fig. 12). Hemipelagic sedimentation began immediately after the knoll's formation and continued throughout the Tertiary. In the early to middle Miocene, subduction at the Nankai Trough slowed and the trench became filled with sediment. Turbidites fed from the Japanese island arc spread more than 700 km out onto the Shikoku Basin and reached the position of KK. Turbidites are present over gentle basement slopes (~ 5–10°) on the northern and western sides of KK, but they are absent on the southeastern side of the knoll, which has relatively steep slopes (~ 20–30°). As the knoll was carried northwestward close to the Nankai Trough, it began to influence the trench sedimentary regime that has been carrying turbidites

down the trench axis from the Izu collision zone in the northeast. Its high topography partially dammed the flow of Quaternary turbidites down the trench axis, forcing the turbidites to flow southward out onto the Shikoku Basin. The knoll is not a westward continuation of ZR and is cut by normal faults rather than the reverse faults that affect Zenisu. As sediment packages above and surrounding KK are carried into the accretionary prism, local variations in sediment type and thickness will lead to rapid along-strike variations in the structure of the accretionary prism.

ACKNOWLEDGEMENTS

REFERENCES

ALEXANDER J. & MORRIS S. 1994. Observations on experimental, nonchannelized, high concentration turbidity currents and variations in deposits around obstacles. *Journal of Sedimentary Research* **A64**, 899–909.

AOIKE K. 1999. Tectonic evolution of the Izu Collision Zone. *Research Report of the Kanagawa Prefectural Museum of Natural History* **9**, 113–51.

AOKI Y., TAMANO T. & KATO S. 1982. Detailed structure of the Nankai Trough from migrated seismic sections. Studies in Continental Margin Geology. *American Association of Petroleum Geologists Memoir* **34**, 309–22.

CADET J. P, KOBAYASHI K., AUBOUIN J. *et al.* 1987. The Japan trench and its juncture with the Kuril trench: Cruise results of the Kaiko project. *Earth and Planetary Science Letters* **83**, 267–84.

CARESS D. W. & CHAYES D. 1996. Improved processing of Hydrosweep DS multibeam data on the R/V Maurice Ewing. *Marine Geophysical Researches* **18**, 631–50.

CHAMOT-ROOKE N., RENARD V. & LE PICHON X. 1987. Magnetic anomalies in the Shikoku basin: A new interpretation. *Earth and Planetary Science Letters* **3**, 214–28.

CLOOS M. & SHREVE R. L. 1996. Shear-zone thickness and the seismicity of Chilean- and Marianas-type subduction zones. *Geology* **24**, 107–10.

DE ROSA R., ZUFFA G. G., TAIRA A. & LEGGETT J. K. 1986. Petrography of trench sands from the Nankai Trough, southwest Japan: Implications for long-distance turbidite transportation. *Geological Magazine* **123**, 477–86.

DOMINGUEZ S., LALLEMAND S. E., MALAVIEILLE J. & VON HUENE R. 1998. Upper plate deformation associated with seamount subduction. *Tectonophysics* **293**, 207–24.

DOMINGUEZ S., MALAVIEILLE J. & LALLEMAND S. E. 2000. Deformation of accretionary wedges in response to seamount subduction: Insights from sandbox experiments. *Tectonics* **19**, 182–96.

FERGUSSON C. L. 2003. Provenance of Miocene, Pleistocene turbidite sands and sandstones, Nankai Trough, Ocean Drilling Program Leg 190. *Proceedings of the Ocean Drilling Program, Scientific Results* **190/196**, 1–28 [online]. [Cited 2008] Available from: http://www-odp.tamu.edu/publications/190196sr/205/205htm

GEOLOGICAL SURVEY OF JAPAN. 1996. *Magnetic Anomaly Map of East Asia* 1:4,000,000 [CD-ROM], Ibaraki, Japan.

GEOLOGICAL SURVEY OF JAPAN. 2000. *Gravity CD-ROM of Japan* [CD-ROM].

HIBBARD J. P. & KARIG D. E. 1990. Alternative plate model for the early Miocene evolution of the Southwest Japan margin. *Geology* **18**, 170–4.

IKE T., MOORE G. F., KURAMOTO S. *et al.* 2008. Variations in sediment thickness and type along the northern Philippine Sea Plate at the Nankai Trough. *Island Arc*, doi:10.1111/j.1440-1738.2008.00624.

ISHII T., SATO H., MACHIDA S. *et al.* 2000. Geological and petrological studies of the Kinan and Izu-Ogasawara-backarc-echelon seamounts Chains. *Bulletin of the Geological Survey of Japan* **51**, 615–30.

KAIZUKA S. 1975. A tectonic model for the morphology of arc-trench systems, especially for the echelon ridges and mid-arc faults. *Japanese Journal of Geology and Geography* **45**, 9–28.

KARIG D. E., INGLE J. C. JR, BOUMA A. H. *et al.* 1975. *Initial Reports of the Deep Sea Drilling Project*, Vol. 31. US Government Printing Office, Washington, DC.

KERR B. C., SCHOLL D. W. & KLEMPERER S. L. 2005. Seismic stratigraphy of Detroit Seamount, Hawaiian-Emperor seamount chain: Post-hot-spot shield-building volcanism and deposition of the Meiji drift. *Geochemistry, Geophysics, and Geosystems* **6**, Q07L10, doi:10.1029/2004GC000705.

KIDO Y. & FUJIWARA T. 2004. Regional variation of magnetization of oceanic crust subducting beneath the Nankai Trough. *Geochemistry, Geophysics, and Geosystems* **5**, Q03002, doi:10.1029/2003GC000649.

KIMURA J., STERN R. J. & YOSHIDA T. 2005. Reinitiation of subduction and magmatic responses in SW Japan during Neogene time. *Geological Society of America Bulletin* **117**, 969–86.

KOBAYASHI K. & NAKADA M. 1978. Magnetic anomalies and tectonic evolution of the Shikoku inter-arc basin, in Geodynamics of the Western Pacific. *Journal of Physical Earth* **26**, 391–402.

KOBAYASHI K., CADET J. P, AUBOUIN J. *et al.* 1987. Normal faulting of Daiichi Kashima Seamount in the Japan Trench revealed by the KAIKO I cruise, Leg 3. *Earth and Planetary Science Letters* **83**, 257–66.

KOBAYASHI K., KASUGA K. & OKINO K. 1995. Shikoku basin and its margins. *In* Taylor B. (ed.). *Backarc Basins: Tectonics and Magmatism*, pp. 381–405. Plenum Press, New York, NY.

KODAIRA S., TAKAHASHI N., NAKANISHI A., MIURA S. & KANEDA Y. 2000. Subducted seamount Imaged in the Rupture Zone of the 1946 Nankaido Earthquake. *Science* **289**, 104–6.

LALLEMANT S. J., CHAMOT-ROOKE N., LE PICHON X. & RANGIN C. 1989. Zenisu Ridge: A deep intraoceanic thrust related to subduction, off Southwest Japan. *Tectonophysics* **160**, 151–74.

LE PICHON X., IIYAMA T., CHAMLEY H. *et al.* 1987. The eastern and western ends of Nankai Trough: Results of box 5 and box 7 Kaiko survey. *Earth and Planetary Science Letters* **83**, 199–213.

MCCANN W. R. & HABERMANN R. E. 1989. Morphologic and geologic effects of the subduction of bathymetric highs. *Pure and Applied Geophysics* **129**, 41–69.

MITCHELL N. C. 2003. Susceptibility of mid-ocean ridge volcanic islands and seamounts to large-scale land-sliding. *Journal of Geophysical Research* **108**, 2397, doi:10.1029/2002JB001997.

MOORE G. F., TAIRA A., KLAUS A. *et al.* 2001. New insights into deformation and fluid flow processes in the Nankai Trough accretionary prism: Results of Ocean Drilling Program Leg 190. *Geochemistry, Geophysics, and Geosystems* **2** doi:10.1029/2001GC000166.

MORGAN J. K., MOORE G. F. & CLAGUE D. A. 2003. Slope failure and volcanic spreading along the submarine south flank of Kilauea volcano, Hawaii. *Journal of Geophysical Research* **108**, 2415, doi:10.1029/2003JB002411.

MUCK M. T. & UNDERWOOD M. B. 1990. Upslope flow of turbidity currents: A comparison among field observations, theory, and laboratory methods. *Geology* **18**, 54–7.

NAKAMURA K., SHIMAZAKI K. & YONEKURA N. 1984. Subduction, bending and education, Present and Quaternary tectonics of the northern border of the Philippine Sea plate. *Bulletin de la Société Géologique de France* **26**, 221–43.

OKINO K. & KATO Y. 1995. Geomorphological study on a clastic accretionary prism: The Nankai Trough. *Island Arc* **4**, 182–98.

OKINO K., OHARA Y., KASUGA S. & KATO Y. 1999. The Philippine Sea: New survey results reveal the structure and the history of the marginal basins. *Geophysical Research Letters* **26**, 2287–90.

OKINO K., SHIMAKAWA Y. & NAGAOKA S. 1994. Evolution of the Shikoku basin. *Journal of Geomagnetism and Geoelectricity* **46**, 463–79.

PARKER R. L. 1991. A theory of ideal bodies for seamount magnetism. *Journal of Geophysical Research* **96**, 16 101–12.

RICCI-LUCCHI G. & CAMERLENGHI A. 1993. Upslope turbiditic sedimentation on the southeastern flank of the Mediterranean ridge. *Bollettino di Oceanologia Teorica Ed Applicata* **11**, 3–25.

SAFFER D. M. & BEKINS B. A. 2002. Hydrologic controls on the morphology and mechanics of accretionary wedges. *Geology* **30**, 271–4.

SANDWELL D. T. & SMITH W. H. F. 1997. Marine gravity anomaly from Geosat and ERS 1 satellite altimetry. *Journal of Geophysical Research* **102**, 10 039–54.

SCHOLZ C. H. & SMALL C. 1997. The effect of seamount subduction on seismic coupling. *Geology* **25**, 487–90.

SENO T., STEIN S. & GRIPP A. E. 1993. A model for motion of the Philippine Sea plate consistent with NUVEL-1 and geological data. *Journal of Geophysical Research* **89**, 941–8.

SOH W., PICKERING K. T., TAIRA A. & TOKUYAMA H. 1991. Basin evolution in the arc-arc Izu collision zone, Mio-Pliocene Miura Group, central Japan. *Journal of the Geological Society (London, U.K.)* **148**, 317–30.

SPINELLI G. A. & UNDERWOOD M. B. 2004. Character of sediments entering the Costa Rica subduction zone: Implications for partitioning of water along the plate interface. *Island Arc* **13**, 432–51.

TAIRA A. 2001. Tectonic evolution of the Japanese island arc system. *Annual Review of Earth and Planetary Sciences* **29**, 109–34.

TAIRA A. & NIITSUMA N. 1986. Turbidite sedimentation in the Nankai Trough as interpreted from magnetic fabric, grain size, and detrital modal analyses. *In* Kagami H., Karig D. E., Coulbourn W. T. *et al.* (eds). *Initial Reports of the Deep Sea Drilling Project*, Vol. 87, pp. 611–32. US Government Printing Office, Washington, DC.

TAIRA A. & CUREWITZ D. (eds). 2005. *CDEX Technical Report*, Vol. 1: *Nankai Trough Seismogenic Zone Site Survey: Kumano Basin Seismic Survey, Philippine Sea, Offshore Kii Peninsula, Japan.* Japan Agency for Marine Earth Science and Technology, Yokohama [online]. [Cited 2008] Available from: http://sio7.jamstec.go.jp/publication

TAIRA A., HILL I., FIRTH J. V. *et al.* 1991. *Proceedings of the Ocean Drilling Program, Initial Reports*, Vol. 131. Ocean Drilling Program, College Station, TX.

TAYLOR B. 1992. Rifting and the volcano-tectonic evolution of the Izu-Bonin-Mariana arc. *In* Taylor B., Fujioka K. *et al.* (eds). *Proceedings of the Ocean*

Drilling Program, Scientific Results, Vol. 126, pp. 627–51. Ocean Drilling Program, College Station, TX.

TAYLOR F. W., MANN P., BEVIS M. G. *et al.* 2005. Rapid forearc uplift and subsidence caused by impinging bathymetric features: Examples from the New Hebrides and Solomon arcs. *Tectonics* **24**, TC6005, doi:10.1029/2004TC001650.

UNDERWOOD M. B., ORR R., PICKERING K. & TAIRA A. 1993. Provenance and dispersal patterns of sediments in the turbidite wedge of Nankai Trough. *In* Hill I. A., Taira A., Firth J. V. *et al.* (eds). *Proceedings of the Ocean Drilling Program, Scientific Results*, Vol. 131, pp. 15–34. Ocean Drilling Program, College Station, TX.

VON HUENE R., RANERO C. R., WEINREBE W. & HINZ K. 2000. Quaternary convergent margin tectonics of Costa Rica, segmentation of the Cocos plate, and Central American volcanism. *Tectonics* **19**, 314–34.

WESSEL P. & SMITH W. H. F. 1995. New version of generic mapping tools released. *Eos Transactions, American Geophysical Union* **76**, 329.

YAMAZAKI T. & OKAMURA Y. 1989. Subducting seamounts and deformation of overriding forearc wedges around Japan. *Tectonophysics* **160**, 207–17.